Heliyon 6 (2020) e03499

Contents lists available at ScienceDirect

Heliyon

journal homepage: www.cell.com/heliyon

Research article

Effects of ultraviolet irradiation with a LED device on bone metabolism associated with vitamin D deficiency in senescence-accelerated mouse P6☆

Daigo Morita [a,b], Yoshitoshi Higuchi [a], Kazuya Makida [a], Taisuke Seki [a], Kunihiro Ikuta [a], Naoki Ishiguro [a], Yoshihiro Nishida [a,*]

[a] Department of Orthopaedic Surgery, Nagoya University Graduate School of Medicine, Nagoya, Aichi, Japan
[b] Department of Orthopaedic Surgery, Hamamatsu Medical Center, Hamamatsu, Shizuoka, Japan

ARTICLE INFO

Keywords:
Physiology
Endocrinology
Musculoskeletal system
Pathology
Metabolism
Osteoporosis
Vitamin D
LED
Bone mineral density

ABSTRACT

Aims: This study investigated effects of narrow-range ultraviolet irradiation (UVR) by a new UV–LED device on vitamin D supply and changes of bone in senescence-accelerated mouse P6 (SAMP6) with vitamin D deficiency.
Main methods: We used female SAMP6 mice as a senile osteoporotic model. We set a total of 3 groups (n = 4 per group); D-UVR+ group (vitamin D deficient–dietary and UVR), D- (vitamin D deficient–dietary), and D+ groups (vitamin D contained–dietary). Mice in the D-UVR + group were UV–irradiated (305nm) with 1 kJ/m^2 twice a week for 12 weeks from 20 to 32 weeks of age. Serum 25(OH)D, 1,25$(OH)_2$D, and micro–computed tomography (CT) were assessed over time. Mechanical test, and histological assay were performed for femurs removed at 32 weeks of age.
Key findings: UVR increased both serum 25(OH)D and 1,25$(OH)_2$D levels at 4 and 8 weeks–UVR in the D-UVR+ group compared with that in the D- group ($P < 0.05$, respectively). Relative levels of trabecular bone mineral density in micro–CT were higher in the D-UVR+ group than in the D- group at 8 weeks–UVR ($P = 0.048$). The ultimate load was significantly higher in the D-UVR+ group than in the D- group ($P = 0.036$). In histological assay, fewer osteoclasts and less immature bone (/mature bone) could be observed in the D-UVR+ group than in the D- group, significantly.
Significance: UVR may have possibility to improve bone metabolism associated with vitamin D deficiency in SAMP6 mice.

1. Introduction

Vitamin D is a molecule that plays an important role in bone metabolism. Clinically, it has been recognized that vitamin D deficiency led to osteomalacia [1] or osteoporosis [2] in adults. Data from clinical randomized, double–blind studies in elderly subjects have reported that vitamin D and calcium improved bone density and significantly reduced fracture risk in subjects [3, 4]. Presently, however, vitamin D insufficiency and deficiency is a global health issue throughout all age groups [5, 6, 7]. Furthermore, it was reported that 87.2% had vitamin D insufficiency of deficiency, especially among the oldest old [8]. Thus, prevention of vitamin D deficiency is an important concern in our modern, increasingly aging society. A new low-cost, conservative or minimally invasive, generally useful treatment for vitamin D deficiency and bone brittleness associated with vitamin D deficiency is required, and could be a valuable tool in the reduction of medical costs.

More than 90% of vitamin D required by humans comes from sun exposure [9, 10]. As the first step in the vitamin D pathway, when the skin is exposed to ultraviolet (UV) light from the sun, previtamin D is synthesized by epidermal 7-dehydrocholesterol (7-DHC). Previtamin D leads to the formation of vitamin D (cholecalciferol) through a thermochemical reaction. Vitamin D is transported to the liver where it is converted to stored 25-hydroxyvitamin [25(OH)D], next, it is converted to the active form, 1,25-dihydroxyvitamin D [1,25$(OH)_2$D], or the inactive form, water-soluble calcitroic acid, in the kidneys [11, 12]. However, although UV exposure is the most important source for vitamin D supply, there are many elderly patients with osteomalacia or osteoporosis who have difficulties in getting enough exposure to sunlight.

☆ Institution at which this work was performed: Department of Orthopaedic Surgery, Nagoya University Graduate School of Medicine, 65 Tsurumai-cho, Showa-ku, Nagoya City 466-8550, Japan.

* Corresponding author.
E-mail address: ynishida@med.nagoya-u.ac.jp (Y. Nishida).

https://doi.org/10.1016/j.heliyon.2020.e03499
Received 10 September 2019; Received in revised form 13 December 2019; Accepted 24 February 2020

UV–light-emitting diodes (UV–LED) device can generate stable narrow-range wavelengths of deep UV light when compared with incandescent or fluorescent UV light. Previously, we reported positive effects of short–term UV irradiation (UVR) on vitamin D supply, and determined effective wavelengths in young mice using this device [13]. However, in this short–term UVR study, we did not observe apparent positive effects on bone morphology in a young mice model. We hypothesized that longer duration of UVR could improve bone morphology in senile osteoporotic bone metabolism. Therefore, the aim of this study was to analyze the effects of long-term UVR with the UV–LED device on vitamin D supply, bone morphology, and bone mechanical strength in senescence-accelerated mouse P6 (SAMP6) with vitamin D deficiency.

2. Material and methods

2.1. Study design

All experimental procedures on animals were approved by the Institutional Animal Utilization Study Committee of Nagoya University (Permit Number; 28106), and were in accordance with the National Institutes of Health Guide for the Care and Use of Laboratory Animals. All experiments were performed under sodium pentobarbital or isoflurane anesthesia, and all efforts were made to minimize suffering. Female 12–week–old SAMP6 mice were fed with a vitamin D–deficient diet until the end of this study (32 weeks of age). The mice were divided into two groups at 20 weeks of age, including a 305nm UV irradiation group (D-UVR+) and a control group (D- group) skin was shaven, without UV irradiation). Another group of control mice was fed with a vitamin D–containing diet from 12 to 30 weeks of age, skin was shaven, without UV irradiation (D+ group). There were three groups with four mice per group. Serum examinations for 25(OH)D and 1,25$(OH)_2$D, and micro–computed tomography (CT) for bone morphology were performed over time during the study period. The mice were sacrificed at 32 weeks of age and specimens were collected for mechanical tests or histological assays (Figure 1).

2.2. Mice and diet

SAMP6 mice were obtained from Japan SLC, Inc. (Hamamatsu, Japan) after approval of the Council for SAM Research (Kyoto, Japan). SAMP6 is an established senile osteoporotic mouse model that spontaneously develops osteoporosis early in life. Osteoporotic change in these mice is characterized by a decrease in osteoblastogenesis and an increase in adipogenesis within the bone marrow, with these features similar to those seen in human senile osteoporosis [14, 15, 16]. The bone phenotype of SAMP6 in a long, tubular bone is thinning of the cortex and trabeculae [14]. Such bone loss is observed at 4 months of age with 5%–10% lower total bone mass and cortical thickness index (CTI) compared with that of normal SAM (SAMR1, SAMR2, SAMP1, and SAMP2). After 4 months of age, the annual loss rate is approximately 2% for CTI and 7% for total bone mass in female mice, although both losses progress gradually. Only female mice were used. Because they are more sensitive to vitamin D production by UVR than male mice [17]. The mice were kept at 25 °C with a 12–h light–dark cycle and shielded from UV light. We used AIN93GA–2 (Oriental Yeast Co ltd., Tokyo, Japan) as the vitamin D–deficient diet and AIN93G as the vitamin D–containing diet [18]. AIN93GA–2 contains no vitamin D, 0.50% calcium, and 7.00% total fat, while AIN93G contains 1000 IU/kg, 0.50%, and 7.00% respectively.

2.3. UV irradiation (UVR)

A surface mount device UV lamps for the LED system, jointly developed by Nikkiso Co. Ltd (Tokyo, Japan) with our research institute, were used as the UV source. For all experiments, we applied a LED module emitting UVB at a 305 nm wavelength, since this is the wavelength closest to UVA that has been shown to have a positive effect on the vitamin D supply in the early stages of UVR [13]. The wave spectrum of this LED module measured using a UV radiometer, USR–45 DA–10 (Ushio Inc., Tokyo, Japan), was demonstrated to be within a very narrow–range [13] (Figure 2). As a previous study described [19], a 2 × 4–cm back patch of skin was cleanly shaved and served as the irradiated area. It is equivalent to approximately 7% of the body surface area [20], which is slightly less than the relative surface area of the unilateral upper limb in humans [21]. Mice were irradiated twice a week in 4 × 6–cm clear acrylic compartments with 1 kJ/m^2 at 0.54 mW/cm^2 of intensity according to a previous study for a total of 12 weeks (from 20 to 32 weeks of age) [13, 22]. The lamps were placed 10 cm above the dorsal patch. Irradiation of 185 s was required. We determined 32 weeks of age as the end point for irradiation because femoral fractures might occur in elderly SAMP6 mice [14]. No obvious complications including erythema of the skin were observed during the irradiation period. In the control (D- and D+) groups, mice (2 × 4–cm shaven skin patch) were illuminated with an incandescent light for the same duration (185 s) and period (12 weeks) as the UV–irradiated mice.

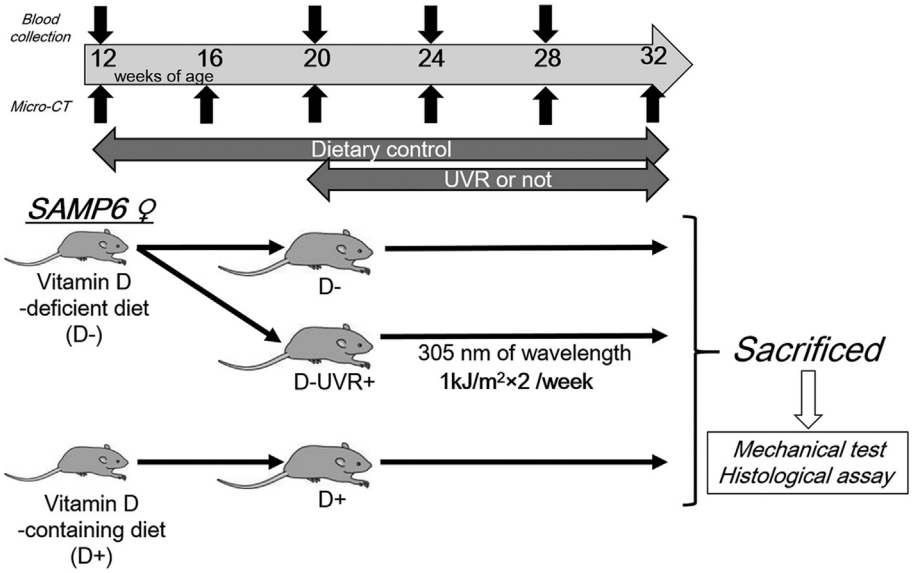

Figure 1. The experimental protocol. The number of mice was four per group. SAMP6, senescence–accelerated mice P6; UV, ultraviolet; UVR+, ultraviolet irradiation; D-, vitamin D–deficient diet; D+, vitamin D–containing diet.

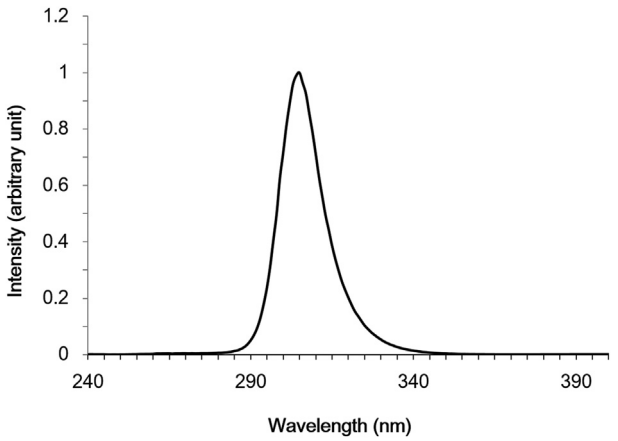

Figure 2. Relative spectral irradiance of a LED module emitting 305 nm wavelength. The wave spectrums and intensity were measured using a UV radiometer.

2.4. Serum metabolites

Blood samples were obtained from the orbital venous plexus at 12, 20 (initiation of UVR), 24 (4–weeks of UVR), and 28 weeks of age (8–weeks of UVR) for four mice in each group (Figure 1). The volume of blood sample at a single collection was 0.2 ml for each mouse. The samples were centrifuged, and the collected serums were protected from room light and stored at −20 °C until quantification. Serum 25(OH)D and $1,25(OH)_2D$ levels were measured using a mini column containing a solid–phase monoclonal antibody followed by radioimmunoassay (RIA) using an ^{125}I–labeled 25(OH)D and $1,25(OH)_2D$ derivative tracer and Sac–cell separation according to the manufacturer's protocol (SRL, Tokyo, Japan) within 3 days after blood collection. The vitamin D levels were classified as follows: deficiency, 25(OH)D < 25 nmol/L; normal, 25 nmol/L ≤ 25(OH)D ≤ 90 nmol/L; sufficiency, 25(OH)D > 90 nmol/L, as a previous study described [23].

2.5. Micro–CT

Micro–CT scans of the right distal femur metaphysis were performed every 4 weeks from 12 to 32 weeks of age for four mice alive in each group (Figure 1) with a high–resolution micro–CT scanner using a specific software (SkyScan 1176; SkyScan, Kontich, Belgium), as previously described [13, 24]. As a brief, each scan was performed with a source voltage of 50 kV, a current of 500 μA, and a 0.5° rotation step, performing as full rotation over 180° with 0.5 mm aluminum filter to reduce beam hardening. The pixel size and exposure time were 9 μm and 0.89 s, respectively. The scan also included a phantom bone to analyze bone mineral density (250 mg/cc and 750 mg/cc) to normalize grayscale values and maintain consistency between runs. Three–dimensional (3D) microstructural image data were reconstructed with a specific software (NRecon, SkyScan) and morphometric parameters were calculated with a specific software (CT Analyzer, SkyScan). To analyze trabecular morphometric parameters, the volume of interest (VOI) started 0.17 mm proximal of the distal growth plate of the femur and extended 2 mm toward the diaphysis, comprising the trabecular bone and the marrow cavity [13, 24]. To examine morphometric parameters of cortical bone, the VOI started at the proximal end of the trabecular VOI and extended 2 mm toward the midshaft, comprising the cortical shell [13]. Trabecular bone parameters [bone volume fraction (Tb.BV/TV, %), trabecular thickness (Tb.Th, μm), spacing (Tb.Sp, mm), number (Tb.N, 1/mm), and bone mineral density (Tb.BMD, mg/cc)], and marrow area (Ma.Ar, mm^2), cortical bone parameters [cortical area (Ct.Ar, mm^2), cortical thickness (Ct.Th, mm), percent cortical area (Ct.Ar/Tt.Ar, %), and bone mineral density (Ct.BMD, mg/cc)] were measured according to guidelines for assessing rodent bone microstructure using micro–CT [25].

2.6. Mechanical test

Mechanical tests of the retrieved right femurs at 32 weeks of age were performed at room temperature using a materials testing machine (MZ500D; Maruto, Tokyo, Japan). The mid–diaphysis of the femur was placed on two supports of the test apparatus located 6 mm apart. The load of a three–point bending test was applied in the anteroposterior direction at the midway point between the two supports. Load–displacement curves were recorded at a crosshead speed of 2.0 mm/s. Mechanical parameters [ultimate load (N), stiffness (N/mm), displacement of fracture (mm), and work to failure (N*mm)] were calculated using CTR win. Ver. 1.05 software (System Supply, Nagano, Japan).

2.7. Bone histology

Retrieved left femurs at 32 weeks of age were fixed in 10% formalin and decalcified. To identify osteoclasts, coronal sections of medial metaphysis of 5 μm in thickness were stained with tartrate–resistant acid phosphatase (TRAP). As a quantitative analysis, osteoclast stained with TRAP in random ten different low magnification fields in the distal metaphysis proximally to the growth plate were measured under a light microscope (magnification 100×). Numbers of osteoclast were counted and divided by the total number of fields. All decalcified specimen were further assessed with Masson's trichrome stain for coronal sections of distal metaphysis of 5 μm in thickness [26]. As a quantitative analysis, the proportions of cartilaginous matrix and fibrous tissue areas as immature bone to mineralized mature bone in random ten different low magnification fields of cortical bone in the distal metaphysis proximally to the growth plate were measured under a light microscope (magnification 100×). The mean proportion of immature bone to mineralized mature bone was calculated by the total number of fields. We determined the number of field for each histological assessments as ten in order to estimate the whole area of distal metaphysis more than twice.

2.8. Evaluation of UV–irradiated skin

Retrieved skin of UV–irradiated area at 32 weeks of age was fixed in 10% formalin. After hematoxylin and eosin staining, widths of epidermis and dermis in random five different low magnification fields were measured under a light microscope (magnification 100×) based on the perpendicular line for the tangent line of the skin surface [27]. For immunohistochemistry, additional tissue sections were stained with rabbit anti–Melan–A monoclonal antibody (ab210546, 1:100 dilution; Abcam, Cambridge, MA, USA) to evaluate melanocyte or keratinocyte with melanin pigmentation. This antibody was confirmed to cross-react with mice antigens by a datasheet provided by the manufacturer. Deparaffinized and rehydrated sections were treated with 0.3% H_2O_2 in methanol for 15 min at room temperature to block the internal peroxidase activity. The sections were incubated over night with rabbit anti–Melan–A monoclonal antibody as a primary antibody using Histofine SAB-PO (M) kit (Nichirei Bioscience, Inc., Tokyo, Japan) at 4 °C. Peroxidase labeling goat anti-rabbit IgG (Nichirei, Tokyo, Japan) was applied as a secondary antibody for 30 min at room temperature, and antibody binding was detected by the addition of diaminobenzidine-containing substrate solution (Nichirei Bioscience, Inc., Tokyo, Japan). Furthermore, we performed Ki67 immunohistochemistry staining for additional tissue sections to examine the effects of UVR on the cell proliferation. Deparaffinized and rehydrated sections were treated with 0.3% H_2O_2 in methanol for 10 min at 4 °C to block the internal peroxidase activity. The sections were incubated for 2 h at room temperature with mouse anti-human Ki67 monoclonal antibody (M7240, 1:100 dilution; Dako, Glostrup, Denmark) as a primary antibody using Histofine SAB-PO (M) kit (Nichirei Bioscience, Inc., Tokyo, Japan). Biotinylated rabbit anti-mouse IgG, IgA, IgM (Nichirei, Tokyo, Japan) was applied as a secondary antibody for 10 min at room temperature, and antibody binding was detected by the addition of streptavidin-peroxidase

reagents and diaminobenzidine-containing substrate solution (Nichirei Bioscience, Inc., Tokyo, Japan).

2.9. Statistics

The results are presented as mean values ± standard deviation. We determined that the number was 4 per group after power and sample size calculations for the unpaired t–test of the difference with a specified power (0.8) and significance level ($P = 0.05$). We used mean levels of serum 25(OH)D of the D-UVR + group at a 305 nm wavelength and the D- group at 1-week of UVR in our previous report [13]. Based on this study, the total mean (SD) level of serum 25(OH)D was set as 55.5 (32.2) nmol/L. The significant difference in serum 25(OH)D level has been estimated as 73.4 nmol/L, according to the difference of mean levels of serum 25(OH)D between both groups. One way analysis of variance followed by post hoc test (Tukey HSD) was used for statistical analyses of results from the micro–CT measurements at 32 weeks of age, mechanical tests, and histological assays. Two way analysis of variance followed by post hoc test (Bonferroni's test) was used for statistical analyses of serum 25(OH)D and $1,25(OH)_2D$ levels, and two way repeated measures analysis of variance followed by post hoc test (Bonferroni's test) was used for statistical analyses of relative levels of main micro–CT parameters. All statistical analyses were performed using SPSS statistics version 23 (IBM Corp. Armonk, NY). Statistical significance was estimated at $P < 0.05$.

3. Results

3.1. Effects of UVR on serum metabolites

Serum 25(OH)D level in the D+ group was nearly the same at each time point. However, the level in the D- group decreased gradually from 12 weeks of age to the deficiency level at 28 weeks of age. At 20 weeks of age, at the initiation of UVR, 25(OH)D levels in the D- and D-UVR+ groups were reduced by 56% and 60% compared to that in the D+ group, respectively (D- group, $P < 0.001$; D-UVR+ group, $P < 0.001$). At 24 and 28 weeks of age, after 4– and 8–weeks of UVR, however, the 25(OH)D level in the D-UVR+ group was almost two times higher than that in the D- group (4–weeks, $P = 0.007$; 8–weeks, $P = 0.002$) (Figure 3a). Serum $1,25(OH)_2D$ level in the D+ group increased over time from 12 to 28 weeks of age. The level in the D- group significantly decreased after 20

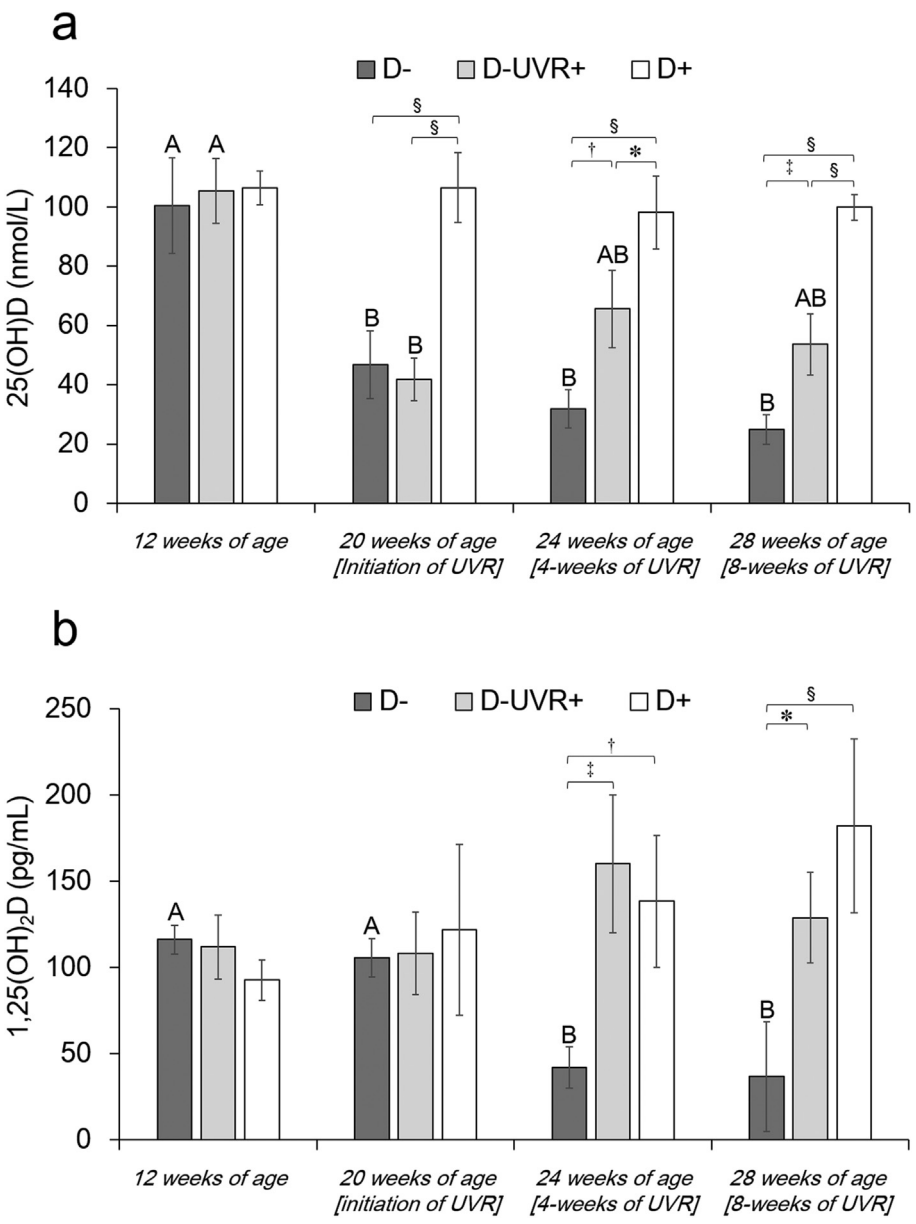

Figure 3. Serum 25(OH)D and $1,25(OH)_2D$ levels. Serum was obtained at 12 weeks of age (initiation of vitamin D–deficient diet or vitamin D–containing diet), 20 weeks of age (initiation of UV irradiation), 24 weeks of age (4–weeks of UV irradiation), and 28 weeks of age (8–weeks of UV irradiation). Obtained serum was tested for 25(OH)D and $1,25(OH)_2D$ levels. Serum levels were analyzed for four mice in each group. a, serum levels of 25(OH)D; b, serum levels of $1,25(OH)_2D$. $^*P < 0.05$, $^{\dagger}P < 0.01$, $^{\ddagger}P < 0.005$, $^{\S}P < 0.001$, and distinct letters ($P < 0.05$) determined by two way analysis of variance (ANOVA) followed by post hoc test (Bonferroni's test). Distinct letters mean statistically significant differences within groups. D-, vitamin D–deficient diet; D+, vitamin D–containing diet; UVR+, ultraviolet irradiation.

weeks of age. However, at 24 and 28 weeks of age, serum 1,25(OH)$_2$D level in the D-UVR+ group was 3.8 and 3.5 times higher than that in the D- group (4–weeks, $P = 0.002$; 8–weeks, $P = 0.013$) (Figure 3b). The results of two way ANOVA for 25(OH)D were as follows: Group: $F_{2,\ 36} = 114.35$, $P < 0.001$; Time: $F_{3,\ 36} = 40.04$, $P < 0.001$; and Group × Time interaction: $F_{6,\ 36} = 10.21$, $P < 0.001$. Those for 25(OH)$_2$D were as follows: Group: $F_{2,\ 36} = 21.08$, $P < 0.001$; Time: $F_{3,\ 36} = 0.18$, $P = 0.91$; and Group × Time interaction: $F_{6,\ 36} = 7.65$, $P < 0.001$.

3.2. Analyses of bone morphology with micro-computed tomography

Regarding trabecular bone parameters, Tb.N in the D-UVR+ and D+ groups were 58% and 75% higher than those in the D- group at 32 weeks of age, respectively (D-UVR+ group, $P = 0.043$; D+ group, $P = 0.028$). There were no significant differences in other trabecular bone parameters among D-, D-UVR+, and D+ groups. As for cortical parameters, there were no significant differences in all parameters among D-, D-UVR+, and D+ groups (Table 1). Regarding relative levels of main parameters based on the values at 12 weeks of age, we observed that Tb.BV/TV, Tb.BMD, and Tb.Th decreased across the duration from 12 to 32 weeks of age (Tb.BV/TV, $F_{5,\ 54} = 97.26$, $P < 0.001$; Tb.BMD, $F_{5,\ 54} = 50.00$, $P < 0.001$; Tb.Th, $F_{5,\ 54} = 28.88$, $P < 0.001$), and Ct.Th increased across the same duration ($F_{5,\ 54} = 3.47$, $P = 0.011$). There were no significant differences among D-, D-UVR+, and D+ groups regarding all main parameters (Tb.BV/TV, $F_{2,\ 54} = 2.12$, $P = 0.183$; Tb.BMD, $F_{2,\ 54} = 2.64$, $P = 0.132$; Tb.Th, $F_{2,\ 54} = 0.71$, $P = 0.522$; Ct.Th, $F_{2,\ 54} = 1.24$, $P = 0.340$). However, the relative level of Tb.BV/TV decreased faster in the D- group than in the D-UVR+ and D+ group ($F_{10,\ 54} = 2.25$, $P = 0.034$). Moreover, only at 28 weeks of age, Tb.BMD was significantly higher in the D-UVR+ and D+ groups than in the D- group (D- group, 47%; D-UVR+ group, 61%, $P = 0.048$; D+ group, 63%, $P = 0.043$) (Figure 4). Figure 5 depicts the extracted 3–dimentional digital images of the right femur in all groups based on micro–CT data at 32 weeks of age.

Table 1. Micro–CT analyses for morphological parameters of trabecular and cortical bone at 32 weeks of age.

Parameters	D-	D-UVR+	D+
Tb.BV/TV (%)	7.1 ± 1.9	13.2 ± 4.5	13.3 ± 4.0
Tb.Th (μm)	60.3 ± 5.9	67.5 ± 10.5	62.2 ± 12.8
Tb.N (1/mm)	1.2 ± 0.2	1.9 ± 0.5*	2.1 ± 0.4*
Tb.Sp (μm)	628.6 ± 191.3	492.8 ± 20.7	492.2 ± 66.2
Tb.BMD (mg/cm^3)	120.1 ± 17.2	154.4 ± 38.4	173.2 ± 39.1
Ct.Ar (mm^2)	1.19 ± 0.05	1.21 ± 0.06	1.21 ± 0.07
Ma.Ar (mm^2)	1.01 ± 0.23	0.93 ± 0.08	0.90 ± 0.03
Ct.Ar/Tt.Ar (%)	54.4 ± 6.1	56.7 ± 2.2	57.3 ± 2.0
Ct.Th (μm)	249.5 ± 25.3	261.7 ± 10.7	264.5 ± 14.3
Ct.BMD (mg/cm^3)	973.3 ± 11.3	980.0 ± 16.4	985.5 ± 8.6

Statistical analyses were performed using by one way analysis of variance followed by post hoc test (Tukey HSD). * $P < 0.05$; v.s. D- group. All parameters were analyzed for four mice in each group. CT, computed tomography; D-, vitamin D–deficient diet; D+, vitamin D–containing diet; UVR+, ultraviolet irradiation; BV, bone volume; TV, tissue volume; Tb.BV/TV, trabecular percent bone volume; Tb.Th, trabecular thickness; Tb.N, trabecular number; Tb.Sp, trabecular separation; Tb.BMD, trabecular bone mineral density; Ct.Ar, cortical area; Ma.Ar, marrow area; Tt.Ar; tissue area; Ct.Ar/Tt.Ar, percent cortical area; Ct.Th, cortical thickness; Ct.BMD, cortical bone mineral density.

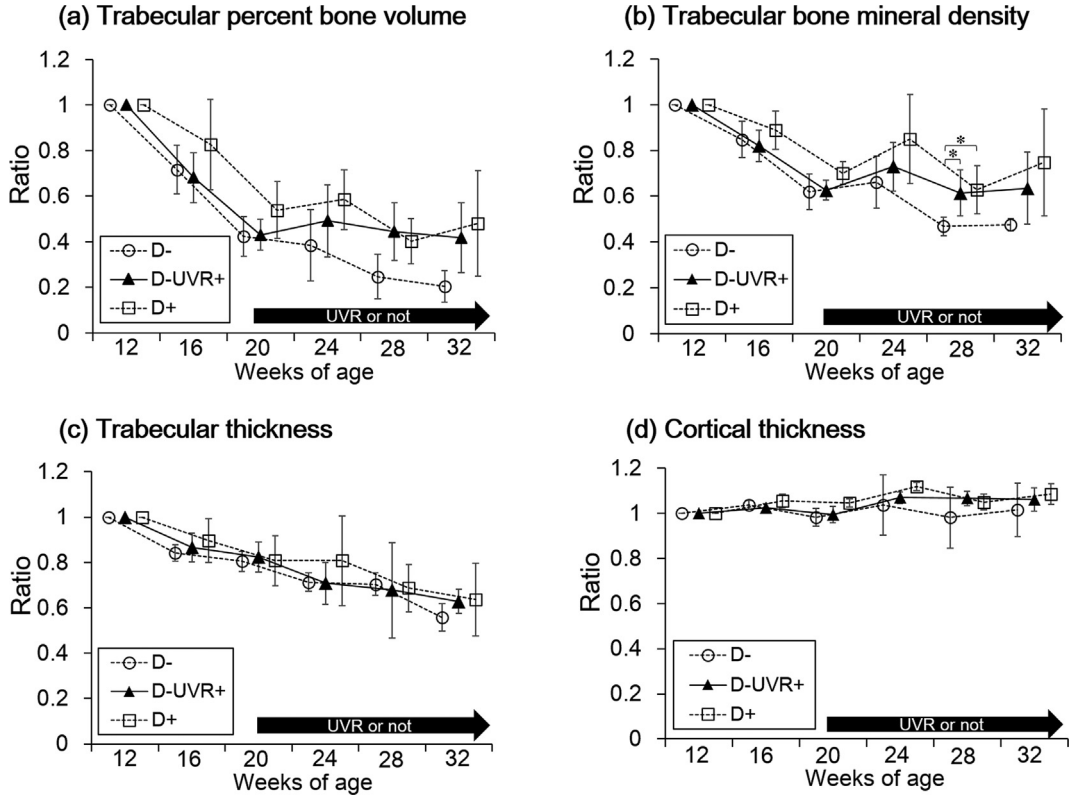

Figure 4. Bone morphological parameters by micro–CT analyses. Relative levels of each parameter determined by micro–CT are compared with the values at 12 weeks of age, set as 1.0. Values of each bone morphological parameter were determined at 12 weeks of age (initiation of vitamin D–deficient diet or vitamin D–containing diet), 16 weeks of age (4 weeks of dietary control), 20 weeks of age (initiation of UV irradiation), 24 weeks of age (4–weeks of UV irradiation), 28 weeks of age (8–weeks of UV irradiation), and 32 weeks of age (12–weeks of UV irradiation). All parameters were analyzed for four mice in each group. a, trabecular percent bone volume [Tb.BV/TV]; b, trabecular bone mineral density [Tb.BMD]; c, trabecular thickness [Tb.Th]; d, cortical thickness [Ct.Th]. *$P < 0.05$ determined by two way repeated measures analysis of variance (ANOVA) followed by post hoc test (Bonferroni's test). CT, computed tomography; D-, vitamin D–deficient diet; D+, vitamin D–containing diet; UVR+, ultraviolet irradiation.

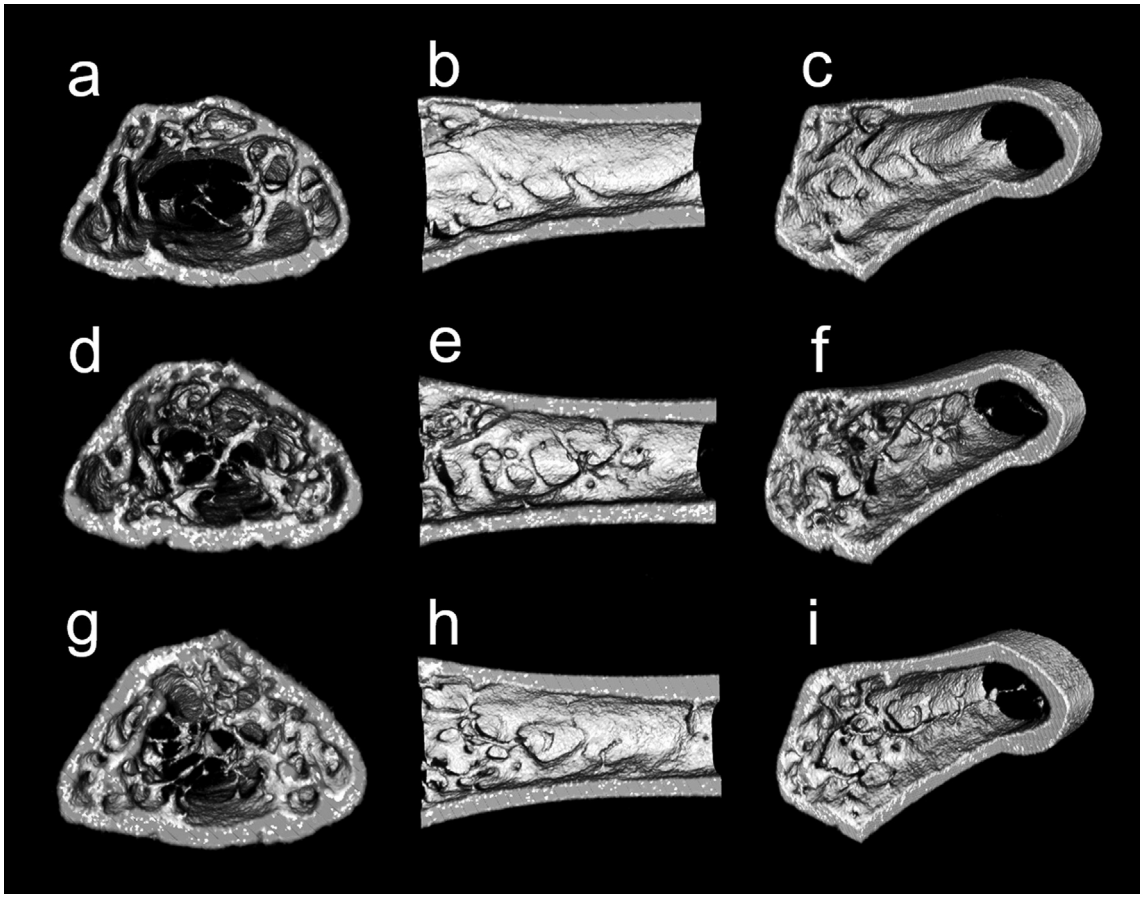

Figure 5. Three–dimensional digital images of right femur. Three–dimensional images of right femur were reconstructed based on micro–CT data at 32 weeks of age mice. a, D- image viewed from a distal viewpoint; b, D- image viewed from a lateral viewpoint; c, D- image viewed from a distal–lateral viewpoint; d, D-UVR+ image viewed from a distal viewpoint; e, D-UVR+ image viewed from a lateral viewpoint; f, D-UVR+ image viewed from a distal–lateral viewpoint; g, D+ image viewed from a distal viewpoint; h, D+ image viewed from a lateral viewpoint; i, D+ image viewed from a distal–lateral viewpoint. The number of trabeculae in the cancellous bone of D- images (a–c) was less compared with that of D-UVR+ (d–f) or D+ images (g–i). Thinning of cortex bone was prominent at metaphysis in the D- image (b), although thickness of cortex bone at the midshaft of D- images (b, c) was equivalent to that of D-UVR+ (e, f) or D+ images (h, i). CT, computed tomography; D-, vitamin D–deficient diet; D+, vitamin D–containing diet; UVR+, ultraviolet irradiation.

3.3. Mechanical parameters of the femur

Between the D-UVR+ and D+ groups, all parameters were approximately equal. Between the D-UVR+ and D- groups, on the other hand, ultimate load in the D-UVR+ group was increased by 11% compared to that in the D- group ($P = 0.036$). There were no significant differences among D-, D-UVR+, and D+ groups regarding stiffness, displacement of fractures, or work to failure (Table 2).

3.4. Bone histology

Mean numbers of osteoclasts in a low magnification field (100×) in the D-UVR+ and D+ groups were reduced by 35% and 56% compared to that in the D- group, respectively (D-UVR+ group, $P < 0.001$; D+ group, $P < 0.001$; Figure 6a–c, g). Furthermore, mean proportions of immature bone in a low magnification field (100×) in the D-UVR+ and D+ groups were reduced by 55% and 43% compared to that in the D- group, respectively (D-UVR+ group, $P < 0.001$; D+ group, $P < 0.001$; Figure 6d–f, h).

3.5. Adverse effects of UVR on skin

Skin epidermal and dermal thickness in the D-UVR+ group was significantly thicker than that in the D- and D+ group (v.s. D- group, $P < 0.001$; v.s. D+ group, $P < 0.001$; Figure 7a–c, j). These differences were more prominent in epidermal thickness than in dermal thickness (Figure 7k, l). Epidermal thickness in the D-UVR+ group was 2.6 and 5.6 times thicker than that in the D- and D+ group. As for immunohistochemistry, there were no melanocytes or keratinocytes with melanin pigmentation at epidermal areas in the D- and D+ groups (Figure 7d, f), although we did observe a few keratinocytes with melanin pigmentation at the border between epidermal and dermal area in the D-UVR+ group (Figure 7e). Furthermore, there were no Ki67-positive cells in all groups (Figure 7g–i).

4. Discussion

Several studies have attempted to improve bone morphology in animal models or human subjects using UVR [13, 28, 29, 30], although many studies have demonstrated that UVR is effective on increasing the supply of vitamin D [13, 28, 29, 30, 31, 32, 33]. Of these studies, only the report by Guo [30] showed that long–term UVR (12–weeks) improved bone mineral content and bone mineral density in young rats. However, it was unclear whether long–term UVR could improve bone morphology in senile osteoporotic bone metabolism. This is the first report demonstrating, through analysis of bone morphology, mechanical strength, and histological evaluation, that UVR by a UV–LED device is effective for the prevention of negative bony changes associated with vitamin D deficiency in senile osteoporotic mice model.

Our previous study did not show any apparent positive effects of UVR on bone morphology [13]. This discrepancy between the results of the present and previous studies may be attributable to the fact that the

Table 2. Results of mechanical test at 32 weeks of age.

Parameters	D-	D-UVR+	D+
Ultimate load (N)	23.5 ± 0.6	26.4 ± 1.7*	24.8 ± 1.6
Stiffness (N/mm)	187.5 ± 10.4	194.4 ± 11.2	206.2 ± 5.6
Displacement of fracture (mm)	0.29 ± 0.04	0.26 ± 0.05	0.26 ± 0.01
Work to failure (N*mm)	4.7 ± 0.8	4.7 ± 1.3	4.5 ± 0.4

Statistical analyses were performed using by one way analysis of variance followed by post hoc test (Tukey HSD). * $P < 0.05$; v.s. D- group. All parameters were analyzed for four mice in each group. D-, vitamin D–deficient diet; D+, vitamin D–containing diet; UVR+, ultraviolet irradiation; N, newton.

periods of the vitamin D–deficient diet and UVR were longer in the present study than those in the previous one. The periods of the vitamin D–deficient diet before UVR and UVR in the present study were 8–weeks and 12–weeks, respectively, while either those in the previous study were 4–weeks. A second explanation may be related to the fact that a senile osteoporotic mouse model was used in this study, while the mice used in the previous study had normal bone metabolism. It was demonstrated that long–term (14 months) vitamin D deficiency in older adult C57BL/6 does not affect bone morphology [34]. However, Duque [35] reported that short–term infusion (6 weeks) of $1,25(OH)_2D$ was effective for preventing osteoporotic, particularly for periosteal ossification and BMD in SAMP6 mice, which supports the results obtained in the present study.

Several *in vivo* studies reported that vitamin D decreases the pool of osteoclast precursor cells [36], and inhibits osteoclast migration into bone based on an original *in vivo* imaging method [37]. Results obtained from TRAP stain in our histological assay showed inhibitory effects of vitamin D on TRAP positive osteoclast expression *in vivo*, which were consistent with the results of previous reports [36, 37]. In this study, changes in trabecular bone parameters resulting from UVR were more apparent than changes in cortical bone parameters. The difference between trabecular and cortical bone may be relevant to variation in bone metabolism according to the matrix volume and surface area. Trabeculae, as thin plates, have a low matrix volume and large surface area. Thus, bone metabolism signals within the matrix can promptly traverse the matrix and locate a surface to initiate trabecular remodeling. By contrast, cortical bone has a large matrix volume and small surface area. Thus, signals deep within the matrix may not locate a surface as readily to initiate remodeling, resulting in the accumulation of micro–damages particularly in interstitial bone that is less remodeled [38, 39]. In line with our results, Duque [35] reported that infusion of $1,25(OH)_2D$ was effective for preventing osteoporotic changes in SAMP6 mice, particularly in trabecular bone rather than cortical bone. Furthermore, results obtained from Masson's trichrome staining showed less immature bone in the D-UVR+ or D+ group than in the D-group. Osteomalacia–like changes caused by long–term vitamin D deficiency could be also prevented by UVR. This may be a reason that mechanical strength in the D-UVR+ group was better than that in the D- group, although Ct.Ths obtained from micro–CT analysis were equivalent between two groups.

More native vitamin D intake or much more sun exposure is recommended to improve the status of vitamin D deficiency [6, 40]. However, it seems to be difficult that the elderly takes in recommended native vitamin D from food, which is at least 20 μg per day [41], and is exposed to more sunlight, particularly in the institutionalized elderly with low mobility. Although native vitamin D supplements may be effective for vitamin D deficiency, the elderly might have difficulty in taking in the adequate level of vitamin D every day even if they took in

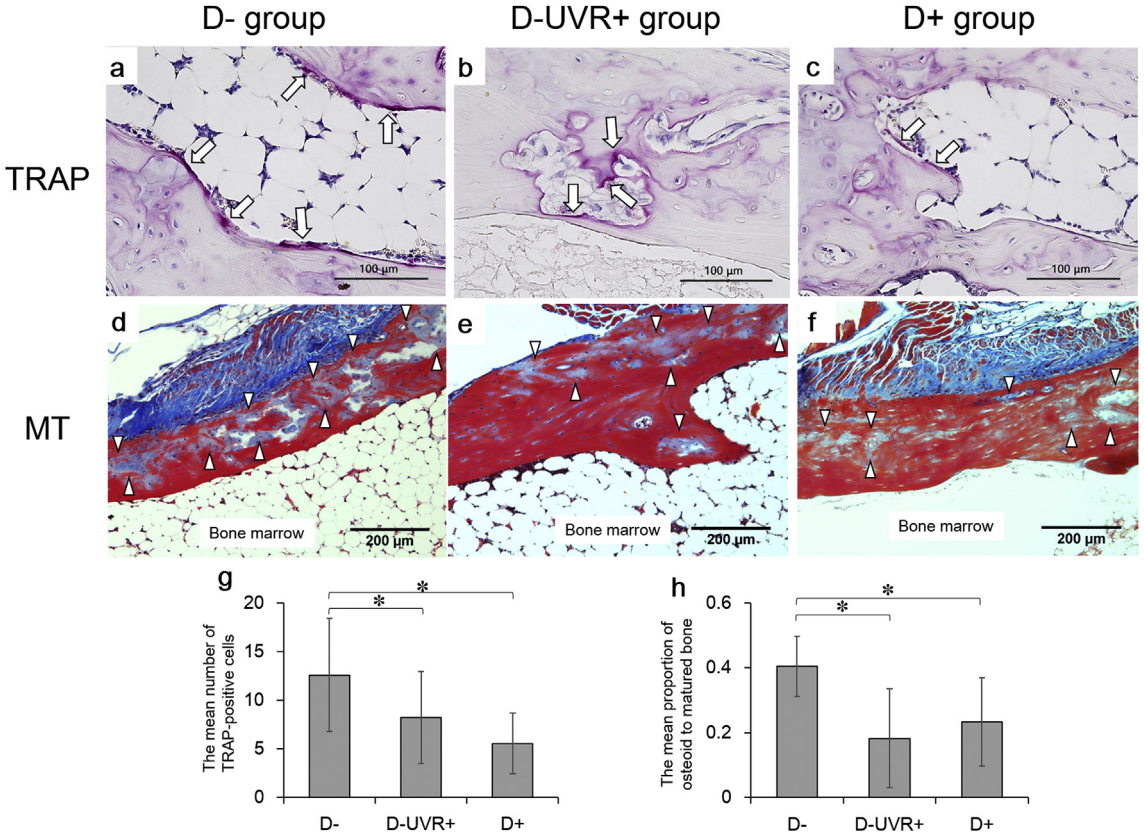

Figure 6. Results of bone histological assays. a–c, tartrate–resistant acid phosphatase (TRAP) stain for coronal sections of medial metaphysis of the left femurs (original magnification 400×, bars indicate 100 μm). White arrows show osteoclasts stained with TRAP. d–f, Masson's trichrome stain for coronal sections of cortical bone of the left femurs (original magnification 100×, bars indicate 200 μm). Immature bone is shown as blue area (white arrow head). g, quantification of TRAP–positive cell numbers in ten low magnification fields (100×). h, quantification of immature bone areas to mineralized mature bone in ten low magnification fields (100×). All parameters were analyzed for four mice in each group. *$P < 0.001$ by one way analysis of variance followed by post hoc test (Tukey HSD). TRAP, tartrate–resistant acid phosphatase stain; MT, Masson's trichrome stain; D-, vitamin D–deficient diet; D+, vitamin D–containing diet; UVR+, ultraviolet irradiation.

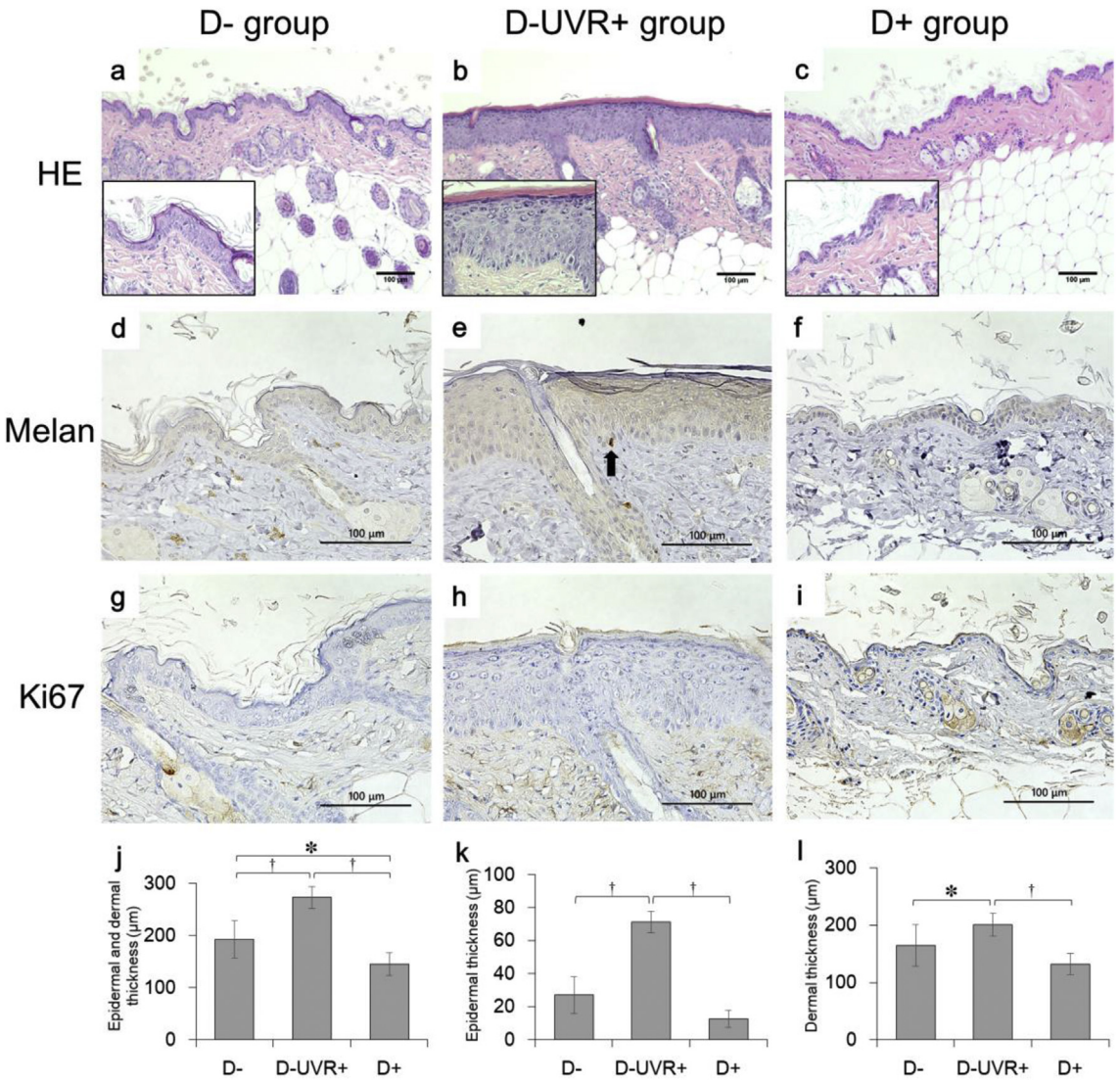

Figure 7. Results of skin histological assays. a–c, hematoxylin and eosin stain for epidermis and dermis, (original magnification 100×, bars indicate 100 μm). d–f, immunohistochemical staining with anti–Melan–A monoclonal antibody for epidermis and dermis (original magnification 400×, bars indicate 100 μm). The black arrow shows a keratinocyte with melanin pigmentation. g–i, immunohistochemical staining with anti–Ki67 monoclonal antibody for epidermis and dermis (original magnification 400×, bars indicate 100 μm). j, quantification of epidermal and dermal thickness in five low magnification fields (100×). k, quantification of epidermal thickness in five low magnification fields (100×). l, quantification of dermal thickness in five low magnification fields (100×). All parameters were analyzed for four mice in each group. $^{*}P < 0.01$, $^{\dagger}P < 0.001$ by one way analysis of variance followed by post hoc test (Tukey HSD). D-, vitamin D–deficient diet; D+, vitamin D–containing diet; UVR+, ultraviolet irradiation; HE, hematoxylin and eosin stain; Melan, immunohistochemical stain with anti–Melan–A monoclonal antibody.

vitamin D with supplements [42]. Moreover, it is an important problem that vitamin D supplements are expensive [43]. As to sun exposure, the same effect could not be provided all the time by difference in location, season, time, and atmospheric conditions [44]. UVR treatment with a UV–LED device has advantages for these problems of vitamin D supplementation and sun exposure. Regarding vitamin D medication, there are several potential risks of negative effects of high–dose vitamin D medication on bone metabolism [45, 46] and hypercalcemia [47]. However, UVR for vitamin D supply could reduce those risks, because levels of active vitamin D [1,25$(OH)_2$D] synthesized endogenously are regulated by renal 1α–hydroxylase and 24–hydroxylase through the homeostatic response to levels of the vitamin D hormone and calcium [11, 13, 48].

In this study, we applied a dose of 1 kJ/m^2 twice a week by using a LED module emitting 305 nm wavelength. This dose was considered as a suberythemal dose [13], and confirmed an increase in serum 25(OH)D levels. However, this dose corresponds to approximately a total dose of UVB from sunlight per day in the summer in Japan (Tsukuba city, 36°N, 140°E) [49]. Vähävihu [50] reported that UVR with narrow–range wavelengths of deep UV around 311 nm for 7 days (100 J/m^2 on the first day and thereafter 200 J/m^2/day) on the head and arms, increased serum 25(OH)D levels in human. Regarding UV wavelength of UVR, according to the reciprocal erythemal action spectrum which was often considered as an index of risk for chronic skin damage, skin aging, and skin cancer [51], those risk ratio was approximately ten times higher in 305 nm wavelength selected in this study than in 316 nm wavelength, which was the boundary wavelength between UVB and UVA. Although skin erythema was not observed during the UVR period in mice, narrow–range UVB irradiation used in the present study had the risk for skin damage. In fact, results obtained from skin histology showed that UVR thickened epidermis and dermis. Furthermore, we observed a few Melan–A positive cells in epidermal areas only in the D-UVR+ group, which were considered to be keratinocytes with melanin pigmentation, although UVR used in this study did not have effects on cell proliferation in epidermis and dermis. Considering the high dose of UVR and the harmful wavelength, the protocol shown in the present study could not be adapted to clinical

use. We reported that UVR with 316 nm wavelength was also effective for vitamin D supply in our previous study [13], although the positive effect was slightly less than other wavelengths of UVB. Patients could avoid unnecessary and harmful UVR wavelengths in vitamin D supply by using a LED module emitting 316 nm wavelength, compared with other lamps of broad–range UV or sunlight. In the future, we plan to evaluate the effects of vitamin D supply and side effects such as DNA damages with various lower doses of UVR than 1 kJ/m^2 twice a week by using 316 nm wavelength, belonging to UVA, as the least harmful one in our modules.

There were several potential limitations in this study. First, we measured only serum 25(OH)D and 1,25$(OH)_2$D levels by RIA, because the volume of blood sample obtained from a mouse was so small that we could not estimate other biochemical parameters. Serum parathyroid hormone, calcium, and phosphate levels, which were closely interacted with vitamin D and bone metabolism, should be measured with serum 25(OH)D and 1,25$(OH)_2$D levels to estimate the effects of UVR on bone metabolism. In a study of 405 women with femoral neck fracture and vitamin D deficiency, Di Monaco [52] reported that secondary hyperparathyroidism associated with vitamin D deficiency was related to bone mineral density, rather than the severity of vitamin D deficiency. We plan to evaluate these biochemical parameters with 25(OH)D and 1,25$(OH)_2$D in the future study for medium–sized animals. Second, the sample size was relatively small. Although we determined the sample size after power and sample size calculations for serum 25(OH)D levels, larger sample size is desirable for assessments of bone morphology, and bone mechanical strength. Furthermore, we did not set another experimental group of mice fed with a vitamin D-containing diet with UVR. It was unknown whether UVR increases vitamin D levels or not in vitamin D replete mice. Further research is warranted to clarify the positive effect of UVR on bone morphology and quality.

5. Conclusion

Long-term UVR delivered by the narrow-range UV–LED device is effective on 1,25$(OH)_2$D supply as well as 25(OH)D in SAMP6 mice with vitamin D deficiency. Furthermore, this UVR treatment may have also possibility to improve bone metabolism associated with vitamin D deficiency in SAMP6 mice. Microscopically, it was demonstrated that UVR had inhibitory effects on TRAP positive osteoclast expression. Considering that many developed countries face an increasingly aged population that is more susceptible to the burdens of bone brittleness associated with vitamin D deficiency, UVR treatment with a UV–LED device may represent a promising novel therapeutic approach to this disease. Further studies for medium–sized animals are warranted before clinical use.

Declarations

Author contribution statement

Daigo Morita: Conceived and designed the experiments; Performed the experiments; Analyzed and interpreted the data; Wrote the paper.

Yoshitoshi Higuchi: Conceived and designed the experiments; Performed the experiments; Wrote the paper.

Kazuya Makida: Performed the experiments; Analyzed and interpreted the data; Wrote the paper.

Taisuke Seki: Conceived and designed the experiments; Wrote the paper.

Kunihiro Ikuta: Performed the experiments; Contributed reagents, materials, analysis tools or data; Wrote the paper.

Naoki Ishiguro: Contributed reagents, materials, analysis tools or data; Wrote the paper.

Yoshihiro Nishida: Conceived and designed the experiments; Analyzed and interpreted the data; Contributed reagents, materials, analysis tools or data; Wrote the paper.

Funding statement

This work was supported by a grant from the Ministry of Education, Culture, Sports, Science and Technology of Japan [Grant–in–Aid for Challenging Exploratory Research 17K19903], and Nagoya University Hospital Funding for Clinical Research.

Competing interest statement

The authors declare no conflict of interest.

Additional information

No additional information is available for this paper.

Acknowledgements

We would like to express our gratitude to Nikkiso Co ltd., Tokyo, Japan for their technical cooperation in developing the therapeutic UV–LED device.

References

[1] R. Ives, M. Brickley, New findings in the identification of adult vitamin D deficiency osteomalacia: results from a large-scale study, Int. J. Paleopathol. 7 (2014) 45–56.
[2] S.J. Chon, Y.K. Koh, J.Y. Heo, J. Lee, M.K. Kim, B.H. Yun, et al., Effects of vitamin D deficiency and daily calcium intake on bone mineral density and osteoporosis in Korean postmenopausal woman, Obstet. Gynecol. Sci. 60 (1) (2017) 53–62.
[3] P. Lips, Vitamin D deficiency and secondary hyperparathyroidism in the elderly: consequences for bone loss and fractures and therapeutic implications, Endocr. Rev. 22 (4) (2001) 477–501.
[4] T. Suda, Y. Ueno, K. Fujii, T. Shinki, Vitamin D and bone, J. Cell. Biochem. 88 (2) (2003) 259–266.
[5] M.F. Holick, The vitamin D deficiency pandemic: approaches for diagnosis, treatment and prevention, Rev. Endocr. Metab. Disord. 18 (2) (2017) 153–165.
[6] N. Tsugawa, K. Uenishi, H. Ishida, R. Ozaki, T. Takase, T. Minekami, et al., Association between vitamin D status and serum parathyroid hormone concentration and calcaneal stiffness in Japanese adolescents: sex differences in susceptibility to vitamin D deficiency, J. Bone Miner. Metabol. 34 (4) (2016) 464–474.
[7] S. Tanaka, T. Kuroda, Y. Yamazaki, Y. Shiraki, N. Yoshimura, M. Shiraki, Serum 25-hydroxyvitamin D below 25 ng/mL is a risk factor for long bone fracture comparable to bone mineral density in Japanese postmenopausal women, J. Bone Miner. Metabol. 32 (5) (2014) 514–523.
[8] C. Matheï, G. Van Pottelbergh, B. Vaes, W. Adriaensen, D. Gruson, J.M. Degryse, No relation between vitamin D status and physical performance in the oldest old: results from the Belfrail study, Age Ageing 42 (2) (2013) 186–190.
[9] D.E. Lawson, A.A. Paul, A.E. Black, T.J. Cole, A.R. Mandal, M. Davie, Relative contributions of diet and sunlight to vitamin D state in the elderly, Br. Med. J. 2 (6185) (1979) 303–305.
[10] E.M. Poskitt, T.J. Cole, D.E. Lawson, Diet, sunlight, and 25-hydroxyvitamin D in healthy children and adults, Br. Med. J. 1 (6158) (1979) 221–223.
[11] M.F. Holick, Vitamin D deficiency, N. Engl. J. Med. 357 (3) (2007) 266–281.
[12] J.A. MacLaughlin, R.R. Anderson, M.F. Holick, Spectral character of sunlight modulates photosynthesis of previtamin D3 and its photoisomers in human skin, Science 216 (4549) (1982) 1001–1003.
[13] D. Morita, Y. Nishida, Y. Higuchi, T. Seki, K. Ikuta, H. Asano, et al., Short-range ultraviolet irradiation with LED device effectively increases serum levels of 25(OH) D, J. Photochem. Photobiol., B 164 (2016) 256–263.
[14] M. Matsushita, T. Tsuboyama, R. Kasai, H. Okumura, T. Yamamuro, K. Higuchi, et al., Age-related changes in bone mass in the senescence-accelerated mouse (SAM). SAM-R/3 and SAM-P/6 as new murine models for senile osteoporosis, Am. J. Pathol. 125 (2) (1986) 276–283.
[15] M. Shimizu, K. Higuchi, S. Kasai, T. Tsuboyama, M. Matsushita, M. Mori, et al., Chromosome 13 locus, Pbd2, regulates bone density in mice, J. Bone Miner. Res. 16 (11) (2001) 1972–1982.
[16] T. Tsuboyama, K. Takahashi, M. Matsushita, H. Okumura, T. Yamamuro, M. Umezawa, et al., Decreased endosteal formation during cortical bone modelling in SAM-P/6 mice with a low peak bone mass, Bone Miner. 7 (1) (1989) 1–12.
[17] S. Gorman, N.M. Scott, D.H. Tan, C.E. Weeden, R.C. Tuckey, J.L. Bisley, et al., Acute erythemal ultraviolet radiation causes systemic immunosuppression in the absence of increased 25-hydroxyvitamin D3 levels in male mice, PloS One 7 (9) (2012), e46006.
[18] L. Mao, Y. Tamura, N. Kawao, K. Okada, M. Yano, K. Okumoto, et al., Influence of diabetic state and vitamin D deficiency on bone repair in female mice, Bone 61 (2014) 102–108.
[19] J.P. McGlade, S. Gorman, J.C. Lenzo, J.W. Tan, T. Watanabe, J.J. Finlay-Jones, et al., Effect of both ultraviolet B irradiation and histamine receptor function on allergic responses to an inhaled antigen, J. Immunol. 178 (5) (2007) 2794–2802.

[20] M.C. Cheung, P.B. Spalding, J.C. Gutierrez, W. Balkan, N. Namias, L.G. Koniaris, et al., Body surface area prediction in normal, hypermuscular, and obese mice, J. Surg. Res. 153 (2) (2009) 326–331.
[21] G.A. Knaysi, G.F. Crikelair, B. Cosman, The rule of nines: its history and accuracy, Plast. Reconstr. Surg. 41 (6) (1968) 560–563.
[22] S. Geldenhuys, P.H. Hart, R. Endersby, P. Jacoby, M. Feelisch, R.B. Weller, et al., Ultraviolet radiation suppresses obesity and symptoms of metabolic syndrome independently of vitamin D in mice fed a high-fat diet, Diabetes 63 (11) (2014) 3759–3769.
[23] R.C. Malley, H.K. Muller, M. Norval, G.M. Woods, Dietary vitamin D alters the response of the skin to UVB-irradiation depending on the genetic background of the mice, Photochem. Photobiol. Sci. 12 (3) (2013) 536–545.
[24] L.M. Coe, S.A. Tekalur, Y. Shu, M.J. Baumann, L.R. McCabe, Bisphosphonate treatment of type I diabetic mice prevents early bone loss but accentuates suppression of bone formation, J. Cell. Physiol. 230 (8) (2015) 1944–1953.
[25] D.W. Dempster, J.E. Compston, M.K. Drezner, F.H. Glorieux, J.A. Kanis, H. Malluche, et al., Standardized nomenclature, symbols, and units for bone histomorphometry: a 2012 update of the report of the ASBMR Histomorphometry Nomenclature Committee, J. Bone Miner. Res. 28 (1) (2013) 2–17.
[26] S.S. Lu, X. Zhang, C. Soo, T. Hsu, A. Napoli, T. Aghaloo, et al., The osteoinductive properties of Nell-1 in a rat spinal fusion model, Spine J. 7 (1) (2007) 50–60.
[27] A. Viros, B. Sanchez-Laorden, M. Pedersen, S.J. Furney, J. Rae, K. Hogan, et al., Ultraviolet radiation accelerates BRAF-driven melanomagenesis by targeting TP53, Nature 511 (7510) (2014) 478–482.
[28] I. Micić, I.H. Jeon, S.H. Park, S.S. Hwa, J.M. Chun, P. Stojiljković, The effect of short-term low-energy ultraviolet B irradiation on bone mineral density and bone turnover markers in postmenopausal women with osteoporosis: a randomized single-blinded controlled clinical trial, Srp. Arh. Celok. Lek. 141 (9-10) (2013) 615–622.
[29] M.K. Watson, A.W. Stern, A.L. Labelle, S. Joslyn, T.M. Fan, K. Leister, et al., Evaluating the clinical and physiological effects of long term ultraviolet B radiation on Guinea pigs (Cavia porcellus), PloS One 9 (12) (2014), e114413.
[30] R. Guo, Y. Du, S. Zhang, H. Liu, Y. Fu, The effects of ultraviolet supplementation to the artificial lighting on rats' bone metabolism, bone mineral density, and skin, J. Photochem. Photobiol., B 188 (2018) 12–18.
[31] S. Simonsen, C.M. Bonefeld, J.P. Thyssen, C. Geisler, L. Skov, Increase in vitamin D but not regulatory T cells following ultraviolet B phototherapy of patients with atopic dermatitis, Acta Derm. Venereol. 99 (2) (2019) 139–145.
[32] H. Ibrahim, M. El Taieb, Z. El Gamel, A.R. El Saied, Effect of narrow-band ultraviolet B on the serum of 25-hydroxyvitamin D in vitiligo patients, J. Cosmet. Dermatol. 17 (5) (2018) 911–916.
[33] T.A. Kalajian, A. Aldoukhi, A.J. Veronikis, K. Persons, M.F. Holick, Ultraviolet B light emitting diodes (LEDs) are more efficient and effective in producing vitamin D3 in human skin compared to natural sunlight, Sci. Rep. 7 (1) (2017) 11489.
[34] K. van der Meijden, J. Buskermolen, H.W. van Essen, T. Schuurman, W.T. Steegenga, E.M. Brouwer-Brolsma, et al., Long-term vitamin D deficiency in older adult C57BL/6 mice does not affect bone structure, remodeling and mineralization, J. Steroid Biochem. Mol. Biol. 164 (2016) 344–352.
[35] G. Duque, M. Macoritto, N. Dion, L.G. Ste-Marie, R. Kremer, 1,25(OH)2D3 acts as a bone-forming agent in the hormone-independent senescence-accelerated mouse (SAM-P/6), Am. J. Physiol. Endocrinol. Metab. 288 (4) (2005) E723–730.
[36] T. Shibata, A. Shira-Ishi, T. Sato, T. Masaki, A. Masuda, A. Hishiya, et al., Vitamin D hormone inhibits osteoclastogenesis in vivo by decreasing the pool of osteoclast precursors in bone marrow, J. Bone Miner. Res. 17 (4) (2002) 622–629.
[37] J. Kikuta, S. Kawamura, F. Okiji, M. Shirazaki, S. Sakai, H. Saito, et al., Sphingosine-1-phosphate-mediated osteoclast precursor monocyte migration is a critical point of control in antibone-resorptive action of active vitamin D, Proc. Natl. Acad. Sci. U. S. A. 110 (17) (2013) 7009–7013.
[38] E. Seeman, Age- and menopause-related bone loss compromise cortical and trabecular microstructure, J. Gerontol. A Biol. Sci. Med. Sci. 68 (10) (2013) 1218–1225.
[39] J. Li, Q. Bao, S. Chen, H. Liu, J. Feng, H. Qin, et al., Different bone remodeling levels of trabecular and cortical bone in response to changes in Wnt/β-catenin signaling in mice, J. Orthop. Res. 35 (4) (2017) 812–819.
[40] A. Kuwabara, N. Tsugawa, K. Tanaka, M. Fujii, N. Kawai, S. Mukae, et al., Improvement of vitamin D status in Japanese institutionalized elderly by supplementation with 800 IU of vitamin D(3), J. Nutr. Sci. Vitaminol. 55 (6) (2009) 453–458.
[41] P. Pludowski, M.F. Holick, W.B. Grant, J. Konstantynowicz, M.R. Mascarenhas, A. Haq, et al., Vitamin D supplementation guidelines, J. Steroid Biochem. Mol. Biol. 175 (2018) 125–135.
[42] Institute of Medicine (US) Committee to Review Dietary Reference Intakes for Vitamin D and Calcium, Dietary Reference Intakes for Calcium and Vitamin D, in: A. Catharine Ross, Christine L. Taylor, Ann L. Yaktine, Heather B. Del Valle (Eds.), National Academies Press (US), Washington (DC), 2011.
[43] A. Maxmen, Nutrition advice: the vitamin D-lemma, Nature 475 (7354) (2011) 23–25.
[44] M. Miyauchi, C. Hirai, H. Nakajima, The solar exposure time required for vitamin D3 synthesis in the human body estimated by numerical simulation and observation in Japan, J. Nutr. Sci. Vitaminol. 59 (4) (2013) 257–263.
[45] J. Sun, B. Sun, W. Wang, X. Han, H. Liu, J. Du, et al., Histochemical examination of the effects of high-dose 1,25(OH)2D3 on bone remodeling in young growing rats, J. Mol. Histol. 47 (4) (2016) 389–399.
[46] G. Grimnes, R. Joakimsen, Y. Figenschau, P.A. Torjesen, B. Almås, R. Jorde, The effect of high-dose vitamin D on bone mineral density and bone turnover markers in postmenopausal women with low bone mass–a randomized controlled 1-year trial, Osteoporos. Int. 23 (1) (2012) 201–211.
[47] Z. Malihi, Z. Wu, A.W. Stewart, C.M. Lawes, R. Scragg, Hypercalcemia, hypercalciuria, and kidney stones in long-term studies of vitamin D supplementation: a systematic review and meta-analysis, Am. J. Clin. Nutr. 104 (4) (2016) 1039–1051.
[48] K.D. Healy, J.B. Zella, J.M. Prahl, H.F. DeLuca, Regulation of the murine renal vitamin D receptor by 1,25-dihydroxyvitamin D3 and calcium, Proc. Natl. Acad. Sci. U. S. A. 100 (17) (2003) 9733–9737.
[49] Reports of integrated UV-B dose by Japan Meteorological Agency (in Japanese). Available from: http://www.data.jma.go.jp/gmd/env/uvhp/uvb_monthave_tsu.html Cited 30 October 2017.
[50] K. Vähävihu, L. Ylianttila, H. Kautiainen, H. Viljakainen, C. Lamberg-Allardt, T. Hasan, et al., Narrowband ultraviolet B course improves vitamin D balance in women in winter, Br. J. Dermatol. 162 (4) (2010) 848–853.
[51] A.F. McKinley, B.L. Deffey, A reference action spectrum for ultraviolet induced erythema in human skin, CIE J. 6 (1987) 17–22.
[52] M. Di Monaco, C. Castiglioni, R. Tappero, Parathyroid hormone response to severe vitamin D deficiency is associated with femoral neck bone mineral density: an observational study of 405 women with hip-fracture, Hormones (Athens) 15 (4) (2016) 527–533.